Dynamical cluster approximation within an augmented plane wave framework: Spectral properties of $SrVO_3$

Hunpyo Lee,[1] Kateryna Foyevtsova,[1] Johannes Ferber,[1] Markus Aichhorn,[2] Harald O. Jeschke,[1] and Roser Valentí[1]
[1]*Institut für Theoretische Physik, Goethe-Universität Frankfurt, Max-von-Laue-Straße 1, 60438 Frankfurt am Main, Germany*
[2]*Institute of Theoretical and Computational Physics, TU Graz, Petersgasse 16, Graz, Austria*
(Received 3 November 2011; revised manuscript received 13 February 2012; published 3 April 2012)

We present a combination of local-density approximation (LDA) with the dynamical cluster approximation (LDA + DCA) in the framework of the full-potential linear augmented plane wave method, and compare our LDA + DCA results for $SrVO_3$ to LDA with the dynamical mean-field theory (LDA + DMFT) calculations as well as experimental observations on $SrVO_3$. We find a qualitative agreement of the momentum resolved spectral function with angle-resolved photoemission spectra (ARPES) and former LDA + DMFT results. As a correction to LDA + DMFT, we observe more pronounced coherent peaks below the Fermi level, as indicated by ARPES experiments. In addition, we resolve the spectral functions in the $\mathbf{K}_0 = (0,0,0)$ and $\mathbf{K}_1 = (\pi,\pi,\pi)$ sectors of DCA, where band insulating and metallic phases coexist. Our approach can be applied to correlated compounds where not only local quantum fluctuations but also spatial fluctuations are important.

DOI: 10.1103/PhysRevB.85.165103 PACS number(s): 71.10.Fd

I. INTRODUCTION

The development of reliable numerical tools for the description of the electronic structure of correlated compounds is one of the most challenging tasks in the condensed-matter community. As an example, transition-metal perovskites with partially filled t_{2g} orbitals are predicted to be conventional metals in the framework of one-electron approaches like density-functional theory (DFT) in the local-density approximation (LDA). Nevertheless, a few perovskite families show a markedly different behavior; $SrVO_3$ and $CaVO_3$ are correlated metals with significant mass enhancement and $LaTiO_3$ displays features of a Mott insulator.[1,2] In all compounds, this anomalous behavior may be caused by correlations resulting from Coulomb repulsion effects. Therefore progress on methods including correlation effects beyond DFT is very desirable.

Dynamical mean-field theory (DMFT)[3–5] takes local quantum fluctuations fully into account but the momentum dependence of the self-energy is neglected. This method has been developed over the last twenty years and successfully describes the metal-to-Mott insulator transition in frustrated systems[6–10] and non-Fermi-liquid behavior in multiorbital systems[11–13] to mention a few examples. On the other hand, it cannot describe such phases as spin-density wave or d-wave superconductivity due to its lack of spatial correlations. In order to overcome these problems the first extension to single-site DMFT are multisite approaches in which the short-range correlations are exactly considered within a cluster.[14–16] Implementations of these approaches are the dynamical cluster approximation (DCA)[14,16] or the cellular DMFT.[15] These approaches capture the spin-density wave formation indicated as a band insulator[17,18] as well as Mott transitions.[19–24] Recently, other implementations including long-range correlations have been developed by considering a perturbation expansion where nonlocal contributions are obtained from the two-particle vertex functions.[25–29]

Recent progress toward a realistic description of correlated systems is the combination of LDA with DMFT[30] (LDA + DMFT). While this approach has proven to be quite successful for the description of spectral properties of transition-metal oxides[2,31–38] and the newly discovered iron-based superconductors,[39–41] effects originating from spatial fluctuations remain inconclusive. Attempts to include short-range spatial fluctuations have been done in the context of the spin-Peierls system TiOCl—where pairing correlations are important—within an Nth-order muffin-tin orbital (NMTO) approach combined with DCA[42] as well as NMTO combined with a variational cluster approach (VCA).[43] In this work, we present an alternative approach where we extend a newly developed implementation of the LDA + DMFT approach[31] in the context of the full potential linearized augmented plane wave (FLAPW)[44] method by including spatial fluctuations within DCA (LDA + DCA), and we investigate the spectral properties of $SrVO_3$ as a test case.

The paper is organized as follows: in Sec. II, we describe our LDA + DCA implementation with a weak-coupling continuous-time quantum Monte Carlo (CT-QMC) algorithm[45–47] for multiorbital systems with multiple sites. In Sec. III, we present results for $SrVO_3$ within LDA + DCA with a cluster of two sites and compare them with single-site LDA + DMFT calculations as well as experimental observations and in Sec. IV we summarize our findings.

II. THEORETICAL FRAMEWORK

A. LDA + DCA in the APW framework

In this work, we extend a recent implementation of LDA + DMFT[31] to LDA + DCA, which includes short-range spatial correlations. We first shortly review the projection operators within the WIEN2K code.[44] The local atomiclike Wannier orbital functions inside an appropriate energy window W can be expanded over the Bloch basis set as

$$\left|\chi^{\alpha,\sigma}_{\mathbf{k},m}\right\rangle = \sum_{\nu\in W} \left\langle \psi^{\sigma}_{\mathbf{k},\nu} \middle| \chi^{\alpha,\sigma}_{m} \right\rangle \left|\psi^{\sigma}_{\mathbf{k},\nu}\right\rangle, \tag{1}$$

where α indicates the correlated atom, ν is the band index, σ is the spin index, and m is the orbital index. Here, $|\psi^{\sigma}_{\mathbf{k},\nu}\rangle$ is the Bloch eigenfunction in the augmented plane wave basis and

the correlated orbital $|\chi_m^{\alpha,\sigma}\rangle$ is given as $|\chi_m^{\alpha,\sigma}\rangle = |u_l^{\alpha,\sigma}(E_l)Y_m^l\rangle$ within the muffin-tin sphere, where E_l are chosen linearization energies, $u_l^{\alpha,\sigma}$ is the radial wave function, and Y_m^l is the spherical harmonic function. The orthonormalized projector operators for the DMFT and DCA self-consistent equations are calculated by

$$P_{m,\nu}^{\alpha,\sigma}(\mathbf{k}) = \sum_{\alpha',m'} \langle u_l^{\alpha',\sigma}(E_l)Y_{m'}^l | \psi_{\mathbf{k},\nu}^{\sigma}\rangle [O(\mathbf{k},\sigma)^{-1/2}]_{m,m'}^{\alpha,\alpha'}, \quad (2)$$

where $O(\mathbf{k},\sigma)_{m,m'}^{\alpha,\alpha'}$ is the overlap function, which is given as

$$O(\mathbf{k},\sigma)_{m,m'}^{\alpha,\alpha'} = \sum_{\nu\in W} \langle \chi_m^{\alpha,\sigma} | \psi_{\mathbf{k},\nu}^{\sigma}\rangle \langle \psi_{\mathbf{k},\nu}^{\sigma} | \chi_{m'}^{\alpha',\sigma}\rangle. \quad (3)$$

For the LDA + DCA self-consistency procedure, the lattice Green's function is given as

$$G_{\nu,\nu'}^{\sigma}(\mathbf{K}+\tilde{\mathbf{k}},i\omega_n) = \frac{1}{i\omega_n + \mu - \epsilon_{\mathbf{K}+\tilde{\mathbf{k}},\nu}^{\sigma} - \Sigma_{\nu,\nu'}^{\sigma}(\mathbf{K}+\tilde{\mathbf{k}},i\omega_n)}, \quad (4)$$

where we have defined $\mathbf{k} = \mathbf{K} + \tilde{\mathbf{k}}$ with $\mathbf{K}$ being the cluster momenta and $\tilde{\mathbf{k}}$ running over each Brillouin zone (BZ) sector. ω_n is the Matsubara frequency, μ is the chemical potential, $\epsilon_{\mathbf{K}+\tilde{\mathbf{k}},\nu}^{\sigma}$ are the Kohn-Sham (KS) eigenvalues, and $\Sigma_{\nu,\nu'}^{\sigma}(\mathbf{K}+\tilde{\mathbf{k}},i\omega_n)$ is the lattice self-energy, which is calculated as an expansion of the cluster self-energy over the Bloch basis set:

$$\Sigma_{\nu,\nu'}^{\sigma}(\mathbf{K}+\tilde{\mathbf{k}},i\omega_n) = \sum_{\alpha,m,m'} P_{\nu,m}^{\alpha,\sigma^*}(\mathbf{K}+\tilde{\mathbf{k}}) \times \Delta\Sigma_{m,m'}^{\sigma,\mathrm{imp}}(\mathbf{K},i\omega_n) P_{m',\nu'}^{\alpha,\sigma}(\mathbf{K}+\tilde{\mathbf{k}}). \quad (5)$$

From the self-energy we need to subtract the contribution to correlations that is already included in the LDA calculation, commonly called double counting (DC) correction,

$$\Delta\Sigma_{m,m'}^{\sigma,\mathrm{imp}}(\mathbf{K},i\omega_n) = \Sigma_{m,m'}^{\sigma,\mathrm{imp}}(\mathbf{K},i\omega_n) - \Sigma_{m,m'}^{\mathrm{dc}}, \quad (6)$$

where $\Sigma_{m,m'}^{\sigma,\mathrm{imp}}(\mathbf{K},i\omega_n)$ is calculated by the continuous time quantum Monte Carlo (CT-QMC) cluster solver and the Dyson's equation. Calculating the DC correction is not possible exactly, but some approximate expressions have been introduced. Here, we use as the double counting correction

$$\Sigma_{m,m'}^{\sigma,\mathrm{dc}} = \delta_{m,m'}\left[U'\left(N_c - \frac{1}{2}\right) - J\left(N_c^{\sigma} - \frac{1}{2}\right)\right], \quad (7)$$

where $U' = U - 2J$, U is the on-site Coulomb interaction, J is the Hund's coupling, and N_c and N_c^{σ} denote the number of total occupied states and spin-resolved occupied states in the correlated orbitals, respectively.[48] The local cluster Green's functions are given as

$$G_{m,m'}^{\sigma,\mathrm{loc}}(\mathbf{K},i\omega_n) = \sum_{\tilde{\mathbf{k}},\nu,\nu'} P_{m,\nu}^{\alpha,\sigma}(\mathbf{K}+\tilde{\mathbf{k}}) \times G_{\nu,\nu'}^{\sigma}(\mathbf{K}+\tilde{\mathbf{k}},i\omega_n) P_{\nu',m'}^{\alpha,\sigma^{*\prime}}(\mathbf{K}+\tilde{\mathbf{k}}), \quad (8)$$

where the summation over $\tilde{\mathbf{k}}$ is calculated in each Brillouin-zone sector. The LDA + DCA self-consistency condition states that these local cluster Green's functions, Eq. (8), have to be equal to the impurity Green's functions as calculated by CT-QMC. The DMFT update of the Weiss field is given by the Dyson's equation as

$$\left[G_{m,m'}^{\sigma,0}(\mathbf{K},i\omega_n)\right]^{-1} = \Sigma_{m,m'}^{\sigma,\mathrm{imp}}(\mathbf{K},i\omega_n) + \left[G_{m,m'}^{\sigma,\mathrm{loc}}(\mathbf{K},i\omega_n)\right]^{-1}. \quad (9)$$

B. Many-body interactions and CT-QMC algorithm

In order to describe the electronic behavior of $SrVO_3$ one has to consider the multiorbital Hubbard Hamiltonian where the interaction term is given by

$$H_I = U\sum_m n_{m\uparrow}n_{m\downarrow} + \sum_{m<n,\sigma}[U' n_{m\sigma}n_{n\bar{\sigma}} + (U'-J)n_{m\sigma}n_{n\sigma} - J' c_{m\sigma}^{\dagger}c_{m\bar{\sigma}}c_{n\bar{\sigma}}^{\dagger}c_{n\sigma} - J' c_{m\sigma}^{\dagger}c_{m\bar{\sigma}}^{\dagger}c_{n\sigma}c_{n\bar{\sigma}}], \quad (10)$$

and m,n denote the t_{2g} orbitals. In order to solve this model we employ a weak-coupling CT-QMC algorithm. While the weak-coupling CT-QMC algorithm can easily treat a multiple number of sites in the cluster, it is difficult to deal with the full rotationally invariant form of the interaction Hamiltonian due to the fermionic sign problem, in contrast to the strong-coupling CT-QMC algorithm.[49,50] Therefore in what follows we shall consider a simplified Hubbard model where the spin-flip and pair-hopping terms in Eq. (10) are neglected ($J' = 0$).

The main idea of the weak-coupling CT-QMC method is to divide the total action S into an unperturbed term S_0 and the interaction term I which is expanded in a Taylor series. The partition function is rewritten as

$$\mathcal{Z} = \sum_k Z_0 \frac{(-I)^k}{k!}\int d\tau_1\cdots d\tau_k \int \mathcal{D}[c,\bar{c}] \times \langle n_{l_1\uparrow}(\tau_1)n_{l_1'\downarrow}(\tau_1)\cdots n_{l_k\uparrow}(\tau_k)n_{l_k'\downarrow}(\tau_k)\rangle, \quad (11)$$

where $\langle n_{l_1\uparrow}(\tau_1)n_{l_1'\downarrow}(\tau_1)\cdots n_{l_k\uparrow}(\tau_k)n_{l_k'\downarrow}(\tau_k)\rangle$ is determined by the noninteracting Green's function and Wick's theorem, k is the perturbation order, $Z_0 = \mathrm{Tr}(Te^{-S_0})$ corresponds to the unperturbed term, and l, l', and τ_k are randomly sampled. I is given as

$$I = \bar{U}\beta NM(2M-1), \quad (12)$$

where β is the inverse temperature, N and M are the number of sites and the number of orbitals in the cluster, respectively, and $\bar{U}$ is one of U, U', or $U'-J$ depending on the operators considered in the random walk in the average $\langle\cdots\rangle$ in Eq. (11). The impurity Green's functions are calculated by numerically averaging Eq. (11).

III. RESULTS

$SrVO_3$, which is thought to be a prototypical paramagnetic correlated metal with intermediate electron-electron interactions, has served in the past as a testing ground for numerous newly developed LDA + DMFT approaches.[2,31–35,38] In $SrVO_3$, the V $3d$ orbitals are split by the crystal field into triply degenerate t_{2g} and doubly degenerate e_g states. The LDA calculations show that the degenerate t_{2g} states of V form bands crossing the Fermi level which are well separated from the e_g bands.

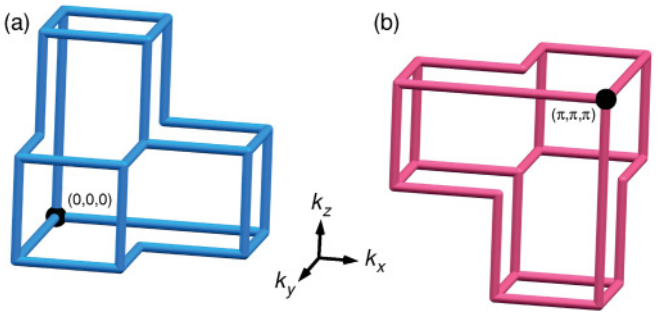

FIG. 1. (Color online) One quadrant of the Brillouin zone of $SrVO_3$. (a) and (b) represent the $\mathbf{K}_0 = (0,0,0)$ and $\mathbf{K}_1 = (\pi,\pi,\pi)$ Brillouin-zone sectors, respectively. Other quadrants follow from symmetry.

For our calculations on $SrVO_3$, we chose the energy window W from -1.35 to 2.0 eV for the t_{2g} orbitals which can then be effectively described by the degenerate three-orbital Hubbard model in Eq. (10). We first reproduced the results of LDA + DMFT from Ref. 31, considering a temperature $T = 0.1$ eV and the same Coulomb interaction $U = 4.0$ eV, and Hund's rule coupling $J = 0.65$ eV. In a next step, we extend the LDA + DMFT solution to LDA + DCA with two sites in the cluster $N = 2$. Within the DCA method, $N = 2$ implies that we have two BZ sectors and the self-energies in the BZ sectors are constant.

The BZ of $SrVO_3$ has cubic symmetry and the self-energies in the cluster momenta $\mathbf{K}_0 = (0,0,0)$ and $\mathbf{K}_1 = (\pi,\pi,\pi)$ are calculated in the BZ sectors shown in Figs. 1(a) and 1(b). In real space, the on-site and nearest-neighbor-site Green's functions are $G_{R=0}(i\omega_n) = \frac{1}{2}[G_{\mathbf{K_0}}(i\omega_n) + G_{\mathbf{K_1}}(i\omega_n)]$ and $G_{R=1}(i\omega_n) = \frac{1}{2}[G_{\mathbf{K_0}}(i\omega_n) - G_{\mathbf{K_1}}(i\omega_n)]$, respectively. Here, the DCA formalism with $N = 2$ for cubic lattice has been clearly presented in Ref. 51. Both on-site and nearest-neighbor-site Green's functions are inserted into the CT-QMC impurity solver, and the LDA + DCA self-consistency is satisfied by Eqs. (8) and (9).

Figure 2(a) shows the density of states $\rho(\omega)$ of the vanadium t_{2g} orbitals obtained within the LDA + DMFT, $\rho(\omega) = A(\omega)$ and LDA + DCA, $\rho(\omega) = \frac{1}{2}[A(\mathbf{K}_0,\omega) + A(\mathbf{K}_1,\omega)]$. Here, the spectral function $A(\mathbf{K},\omega)$ is given as

$$A(\mathbf{K},\omega) = -\frac{1}{\pi}\mathrm{Im}G_{\mathbf{K}}(\omega), \tag{13}$$

and an analytical continuation of the impurity Green's functions is performed through a maximum entropy method. Our LDA + DMFT results obtained by both the weak-coupling CT-QMC[45,46] as well as the strong-coupling CT-QMC algorithms from the ALPS code[52,53] agree with former LDA + DMFT calculations.[2,31,33–35] In Figs. 2(b) and 2(c) we present the spectral functions for the $\mathbf{K}_0 = (0,0,0)$ and $\mathbf{K}_1 = (\pi,\pi,\pi)$ sectors within LDA and LDA + DCA. The new features obtained in LDA + DCA are a broad peak around 1.5 eV and a coherent peak around 0.2 eV below E_F. LDA results [see Fig. 2(b)] as well as most former LDA + DMFT results [see also Fig. 2 (a)] exhibit neither a broad peak nor a clear coherent peak below E_F. Recent angle-resolved photoemission (ARPES) experiments,[54] have observed, in fact, a broad peak around 1.5 eV and a coherent peak around 0.4 eV below E_F

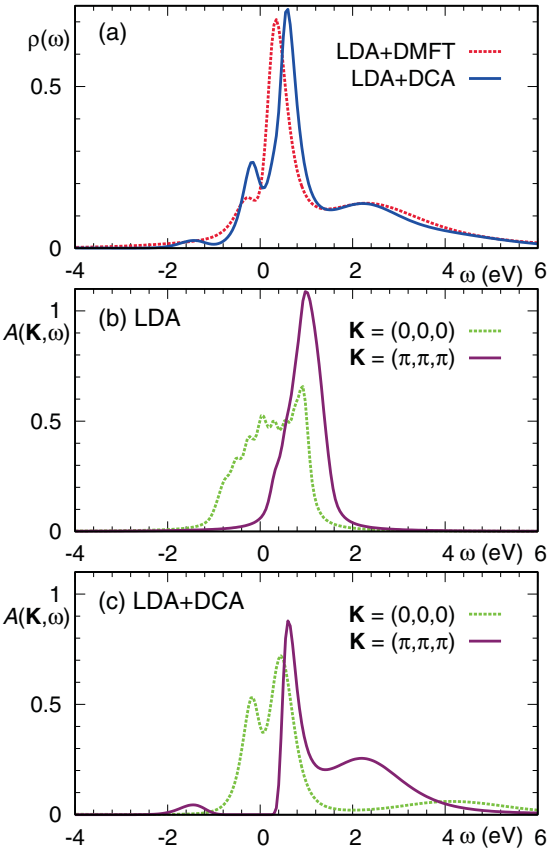

FIG. 2. (Color online) (a) The density of states $\rho(\omega)$ of $SrVO_3$ calculated within the LDA + DMFT and LDA + DCA approaches, with $U = 4.0$ eV, $J = 0.65$ eV, and $T = 0.1$ eV. The density of states $\rho(\omega)$ for LDA + DCA is calculated by $\rho(\omega) = \frac{1}{2}[A(\mathbf{K}_0,\omega) + A(\mathbf{K}_1,\omega)]$, with $\mathbf{K}_0 = (0,0,0)$ and $\mathbf{K}_1 = (\pi,\pi,\pi)$ sectors. (b) and (c) The spectral functions $A(\mathbf{K},\omega)$ obtained from LDA and LDA + DCA for the $\mathbf{K}_0$ and $\mathbf{K}_1$ sectors by Eq. (8), respectively. All the density of states and spectral functions are normalized to 1.

[Fig. 3(b) in Ref. 54]. We suggest that the better agreement of the LDA + DCA with ARPES observations is a consequence of the inclusion of short-range spatial correlations. Figure 2(c) shows that the coherent and broad peaks below the Fermi level are caused by the distinct spectral weights in the $\mathbf{K}_0 = (0,0,0)$ and $\mathbf{K}_1 = (\pi,\pi,\pi)$ sectors. These two sectors also show, respectively, metallic and band insulating behavior reminiscent of the LDA results in these sectors [Fig. 2(b) and Ref. 55].

In Figs. 3(a) and 3(b), we show the momentum resolved spectral functions calculated from Eqs. (4) and (8). The analytical continuation of the self-energy $\Sigma(\mathbf{K},i\omega_n)$ is performed by the maximum entropy approach with subtraction of the Hartree-Fock term.[56] In view of the ill-posed problem of the analytical continuation of the self-energy,[57] we also compared the DOS obtained from integration of the spectral functions with those in Fig. 2(a) and found a reasonable agreement. We also compare LDA + DMFT to LDA + DCA results. One can observe some redistribution of momentum resolved spectral weight between the LDA + DMFT and LDA + DCA results. In Figs. 3(c) and 3(d) we plot the LDA + DMFT and LDA + DCA spectral functions, respectively, in the region between $k_y = -0.6\frac{\pi}{a}$ and $0.4\frac{\pi}{a}$ at $k_x = 0.0$ and $k_z = 0.32\frac{\pi}{a}$

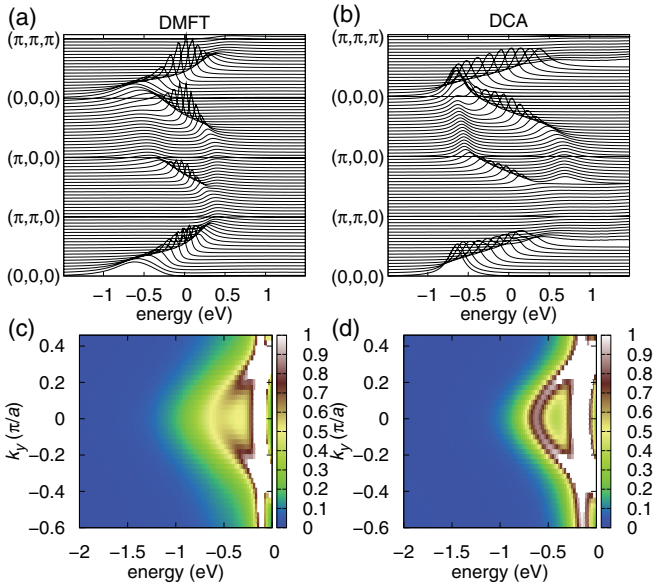

FIG. 3. (Color online) (a) and (b) Spectral functions obtained within (a) LDA + DMFT and (b) LDA + DCA for the vanadium t_{2g} bands. (c) and (d) Spectral functions in the regime between $k_y = -0.6\frac{\pi}{a}$ and $0.4\frac{\pi}{a}$ at $k_x = 0.0$ and $k_z = 0.32\frac{\pi}{a}$ within (c) LDA + DMFT and (d) LDA + DCA for the vanadium t_{2g} bands.

(a is the lattice constant) in order to directly compare our calculations to the ARPES results [Fig. 1(a) of Ref. 54]. In agreement with ARPES experiments, both LDA + DMFT and LDA + DCA show dispersive features around −0.7 though they are more pronounced in the LDA + DCA calculations. Also, the LDA + DCA calculations reproduce the small peak observed around −0.2 eV. These results account for the renormalization of the bands due to electronic correlations.

Finally, our estimation of the mass enhancement is $m^*/m \approx 1.7 \pm 0.3$ within LDA + DMFT and 1.6 ± 0.5 within LDA + DCA at $\mathbf{K}_0 = (0,0,0)$. These values are obtained from

$$m^*/m \approx 1 - \left.\frac{\partial \mathrm{Im}\Sigma(i\omega_n)}{\partial \omega}\right|_{\omega \to 0^+}, \qquad (14)$$

where the derivative is extracted by fitting a third-order polynomial to the lowest four Matsubara frequencies.[58] Note that our LDA + DCA estimates give a slightly smaller mass enhancement than LDA + DMFT estimates with a larger error bar. Both sets of results are in accordance with ARPES estimates of $m^*/m \approx 1.8 \pm 0.2$.[59]

IV. CONCLUSIONS

In conclusion, we have presented an implementation of the LDA + DCA method within the linear augmented plane wave framework. We have compared our benchmark results on $SrVO_3$, which is modeled in terms of a three-band Hubbard Hamiltonian, with earlier LDA + DMFT calculations as well as experimental data. Since the LDA + DCA approach considers both local quantum as well as short-range spatial fluctuations, it offers a more complete description of correlated materials compared to the LDA + DMFT approach, where only local quantum fluctuations are taken into account.

Unlike the LDA + DMFT, the LDA + DCA approach reproduces both coherent and broad peaks for $SrVO_3$ below the Fermi level, observed in angle integrated photoemission experiments. The analysis of the spectral functions at $\mathbf{K}_0 = (0,0,0)$ and $\mathbf{K}_1 = (\pi,\pi,\pi)$ reveals the source of these peaks. While the broad peak is due to the spectral function in the $\mathbf{K}_0 = (0,0,0)$ sector, the coherent peak has its origin in the spectral function at the $\mathbf{K}_1 = (\pi,\pi,\pi)$ sector. We also observe a metallic and a band insulating state at the $\mathbf{K}_0 = (0,0,0)$ and $\mathbf{K}_1 = (\pi,\pi,\pi)$ sectors, also present in the LDA results.

In summary, we believe that the presented LDA + DCA approach is very promising and can be applied to a large variety of multiorbital correlated compounds at different fillings.

ACKNOWLEDGMENTS

We would like to thank Y.-Z. Zhang and C. Gros for useful discussions and we gratefully acknowledge financial support from the Deutsche Forschungsgemeinschaft through Grants No. FOR 1346 (H.L.) and No. SPP 1458 (J.F.) and from the Helmholtz Association through Grant No. HA216/EMMI. M.A. acknowledges support from the Austrian Science Fund, Project No. F4103, and hospitality at Goethe-Universität Frankfurt.

[1] M. Imada, A. Fujimori, and Y. Tokura, Rev. Mod. Phys. **70**, 1039 (1998).
[2] E. Pavarini, S. Biermann, A. Poteryaev, A. I. Lichtenstein, A. Georges, and O. K. Andersen, Phys. Rev. Lett. **92**, 176403 (2004).
[3] W. Metzner and D. Vollhardt, Phys. Rev. Lett. **62**, 324 (1989).
[4] A. Georges, G. Kotliar, W. Krauth, and M. J. Rozenberg, Rev. Mod. Phys. **68**, 13 (1996).
[5] G. Kotliar and D. Vollhardt, Phys. Today **57**(3), 53 (2004).
[6] A. Liebsch, Phys. Rev. Lett. **95**, 116402 (2005).
[7] A. Koga, N. Kawakami, T. M. Rice, and M. Sigrist, Phys. Rev. Lett. **92**, 216402 (2004).
[8] K. Inaba, A. Koga, S.-I. Suga, and N. Kawakami, Phys. Rev. B **72**, 085112 (2005).
[9] R. Zitzler, N-H. Tong, T. Pruschke, and R. Bulla, Phys. Rev. Lett. **93**, 016406 (2004).
[10] H. Lee, Y. Z. Zhang, H. O. Jeschke, and R. Valentí, Phys. Rev. B **81**, 220506(R) (2010).
[11] S. Biermann, L. de'Medici, and A. Georges, Phys. Rev. Lett. **95**, 206401 (2005).
[12] P. Werner, E. Gull, M. Troyer, and A. J. Millis, Phys. Rev. Lett. **101**, 166405 (2008).
[13] H. Ishida and A. Liebsch, Phys. Rev. B **81**, 054513 (2010).
[14] M. H. Hettler, A. N. Tahvildar-Zadeh, M. Jarrell, T. Pruschke, and H. R. Krishnamurthy, Phys. Rev. B **58**, 7475(R) (1998).
[15] G. Kotliar, S. Y. Savrasov, G. Palsson, and G. Biroli, Phys. Rev. Lett. **87**, 186401 (2001).

[16]T. Maier, M. Jarrell, T. Pruschke, and M. H. Hettler, Rev. Mod. Phys. **77**, 1027 (2005).
[17]S. Moukouri and M. Jarrell, Phys. Rev. Lett. **87**, 167010 (2001)
[18]B. Kyung, J. S. Landry, D. Poulin, and A. M. S. Tremblay, Phys. Rev. Lett. **90**, 099702 (2003).
[19]H. Park, K. Haule, and G. Kotliar, Phys. Rev. Lett. **101**, 186403 (2008).
[20]H. Lee, G. Li, and H. Monien, Phys. Rev. B **78**, 205117 (2008).
[21]E. Gull, P. Werner, X. Wang, M. Troyer, and A. Millis, Europhys. Lett. **84**, 37009 (2008).
[22]Y. Z. Zhang and M. Imada, Phys. Rev. B **76**, 045108 (2007).
[23]H. Lee, Y. Z. Zhang, H. O. Jeschke, R. Valentí, and H. Monien, Phys. Rev. Lett. **104**, 026402 (2010).
[24]A. Liebsch, H. Ishida, and J. Merino, Phys. Rev. B **79**, 195108 (2009).
[25]A. Toschi, A. A. Katanin, and K. Held, Phys. Rev. B **75**, 045118 (2007).
[26]A. Toschi, G. Rohringer, A. A. Katanin, and K. Held, Ann. Phys. (Berlin) **523**, 698 (2011).
[27]A. N. Rubtsov, M. I. Katsnelson, and A. I. Lichtenstein, Phys. Rev. B **77**, 033101 (2008).
[28]G. Li, H. Lee, and H. Monien, Phys. Rev. B **78**, 195105 (2008).
[29]H. Hafermann, G. Li, A. N. Rubtsov, M. I. Katsnelson, A. I. Lichtenstein, and H. Monien, Phys. Rev. Lett. **102**, 206401 (2009).
[30]G. Kotliar, S. Y. Savrasov, K. Haule, V. S. Oudovenko, O. Parcollet, and C. A. Marianetti, Rev. Mod. Phys. **78**, 865 (2006).
[31]M. Aichhorn, L. Pourovskii, V. Vildosola, M. Ferrero, O. Parcollet, T. Miyake, A. Georges, and S. Biermann, Phys. Rev. B **80**, 085101 (2009).
[32]A. Liebsch, Phys. Rev. Lett. **90**, 096401 (2003).
[33]B. Amadon, F. Lechermann, A. Georges, F. Jollet, T. O. Wehling, and A. I. Lichtenstein, Phys. Rev. B **77**, 205112 (2008).
[34]M. Karolak, T. O. Wehling, F. Lechermann, and A. I. Lichtenstein, J. Phys.: Condens. Matter **23**, 085601 (2011)
[35]J. Kunes, R. Arita, P. Wissgott, A. Toschi, H. Ikeda, and K. Held, Comput. Phys. Commun. **181**, 1888 (2010).
[36]I. A. Nekrasov, G. Keller, D. E. Kondakov, A. V. Kozhevnikov, Th. Pruschke, K. Held, D. Vollhardt, and V. I. Anisimov, Phys. Rev. B **72**, 155106 (2005).
[37]F. Lechermann, A. Georges, A. Poteryaev, S. Biermann, M. Posternak, A. Yamasaki, and O. K. Andersen, Phys. Rev. B **74**, 125120 (2006).
[38]I. A. Nekrasov, K. Held, G. Keller, D. E. Kondakov, Th. Pruschke, M. Kollar, O. K. Andersen, V. I. Anisimov, and D. Vollhardt, Phys. Rev. B **73**, 155112 (2006).
[39]P. Werner, M. Casula, T. Miyake, F. Aryasetiawan, A. Millis, and S. Biermann, Nat. Phys., advance online publication (2012), doi:10.1038/nphys2250.
[40]Z. P. Yin, K. Haule, and G. Kotliar, Nat. Mater. **10**, 932 (2011).
[41]M. Aichhorn, S. Biermann, T. Miyake, A. Georges, and M. Imada, Phys. Rev. B **82**, 064504 (2010).
[42]T. Saha-Dasgupta, S. Glawion, M. Sing, R. Claessen, and R. Valentí, New J. Phys. **9**, 380 (2007).
[43]M. Aichhorn, T. Saha-Dasgupta, R. Valentí, S. Glawion, M. Sing, and R. Claessen, Phys. Rev. B **80**, 115129 (2009).
[44]P. Blaha, K. Schwarz, G. Madsen, D. Kvasnicka, and J. Luitz, WIEN2k, An Augmented Plane Wave + Local Orbitals Program for Calculating Crystal Properties (Karlheinz Schwarz, Techn. Universität Wien, Austria, 2001).
[45]A. N. Rubtsov, V. V. Savkin, and A. I. Lichtenstein, Phys. Rev. B **72**, 035122 (2005).
[46]F. F. Assaad and T. C. Lang, Phys. Rev. B **76**, 035116 (2007).
[47]E. Gull, A. Millis, A. Lichtenstein, A. Rubtsov, M. Troyer, and P. Werner, Rev. Mod. Phys. **83**, 349 (2011).
[48]V. Anisimov, F. Aryasetiawan, and A. Lichtenstein, J. Phys.: Condens. Matter **9**, 767 (1997).
[49]P. Werner, A. Comanac, Luca de'Medici, M. Troyer, and A. J. Millis, Phys. Rev. Lett. **97**, 076405 (2006).
[50]P. Werner and A. J. Millis, Phys. Rev. B **74**, 155107 (2006).
[51]C. Lin and A. J. Millis, Phys. Rev. B **79**, 205109 (2009).
[52]B. Bauer, L. D. Carr, H. G. Evertz, A. Feiguin, J. Freire, S. Fuchs, L. Gamper, J. Gukelberger, E. Gull, S. Guertler, A. Hehn, R. Igarashi, S. V. Isakov, D. Koop, P. N. Ma, P. Mates, H. Matsuo, O. Parcollet, G. Pawlowski, J. D. Picon, L. Pollet, E. Santos, V. W. Scarola, U. Schollwöck, C. Silva, B. Surer, S. Todo, S. Trebst, M. Troyer, M. L. Wall, P. Werner, and S. Wessel, J. Stat. Mech. (2011) 05001.
[53]E.Gull, P.Werner, S. Fuchs, B. Surer, T. Pruschke, and M. Troyer, Comp. Phys. Commun. **182**, 1078 (2011).
[54]T. Yoshida, M. Hashimoto, T. Takizawa, A. Fujimori, M. Kubota, K. Ono, and H. Eisaki, Phys. Rev. B **82**, 085119 (2010).
[55]H. Wadati, T. Yoshida, A. Chikamatsu, H. Kumigashira, M. Oshima, H. Eisaki, Z. Shen, T. Mizokawa, and A. Fujimori, Phase Transit. **79**, 617 (2006).
[56]K. Chen, S. Pathak, S. Yang, S. Su, D. Galanakis, K. Mikelsons, M. Jarrell, and J. Moreno, Phys. Rev. B **84**, 245107 (2011).
[57]X. Wang, E. Gull, L. de'Medici, M. Capone, and A. J. Millis, Phys. Rev. B **80**, 045101 (2009).
[58]J. Mravlje, M. Aichhorn, T. Miyake, K. Haule, G. Kotliar, and A. Georges, Phys. Rev. Lett. **106**, 096401 (2011).
[59]T. Yoshida, K. Tanaka, H. Yagi, A. Ino, H. Eisaki, A. Fujimori, and Z. X. Shen, Phys. Rev. Lett. **95**, 146404 (2005).